Modeling the Electrochemical Response of Mesoporous Materials Toward Its Application to Biomolecular Detection

Ana Sol Peinetti, Graciela A. González, Fernando Battaglini**

INQUIMAE – Departamento de Química Inorgánica, Analítica y Química Física, Facultad de Ciencias Exactas y Naturales, Universidad de Buenos Aires, Ciudad Universitaria, Pabellón 2, C1428EHA Buenos Aires, Argentina
*e-mail: graciela@qi.fcen.uba.ar; battagli@qi.fcen.uba.ar

Received: November 25, 2009
Accepted: January 12, 2010

Abstract
The performance of an electrochemical sensor based on the ability of a probe to cross a mesoporous membrane partially blocked by an analyte is predicted using a numerical model. The system comprehends a membrane placed close to the working electrode and the signal is generated by applying square wave voltammetry. The digital simulation allows comparing the responses for different situations regarding the way in which the membrane is blocked by the sample. The developed model is compared with experimental results. The effect of the sizes of the pore, analyte and probe on the system response is evaluated.

Keywords: Mesoporous membranes, Digital simulation, Square wave voltammetry, Label-free sensing, Amperometric sensors, Membranes, Sensors

DOI: 10.1002/elan.200900572

1. Introduction

The use of computational models in the design of sensors is an increasing area of interest. In their design two main issues have to be taken into account to model their behavior; on one hand the interaction between recognition agent and analyte, for example docking properties in molecular imprinting systems [1 – 3] or reaction rates between enzymes and substrate [4, 5]. While from the point of view of signal transduction, the used technique has to be considered; for example, in amperometric sensors issues regarding electron transfer properties, mass transport and capacitive effect have to be taken into account [6 – 9].

Mesoporous systems have been presented in different formats as a potential tool for the detection of analytes at very low concentrations by simply using a common property to all molecules, its size [9 – 13]. These systems, combined with a recognition agent, are label-free sensors useful to detect practically any molecule, providing the adequate pore size. Even though all this potential, most of the works presented in the literature have generally shown the proof of concept, and little work has been carried out to optimize the system in order to develop an useful tool for the determination of species at low concentrations. Our group has begun a systematic work regarding the design of sensors based on mesoporous membranes [9]; among the parameters to take into account are: the signal generation, the reproducibility of the assembled system, and the coverage extension of the membrane by the analyte. In most of the works [9, 11, 12] cyclic voltammetry (CV) is used for signal generation, which is an excellent technique for mechanistic studies, but a poor one for quantitative determination due to a relative important capacitive background signal when low concentrations or fast scan rates are used. More appropriate techniques to quantify an electroactive species are those based in pulse voltammetry. Among them, square wave voltammetry (SWV) combines the best aspects of several pulse voltammetric methods, including the background suppression and sensitivity of differential pulse voltammetry. From the advent of fast and software driven potentiostats, square wave voltammetry is becoming a standard technique [14]. As other electrochemical techniques, the method has a supporting theory [15, 16]; however, the response modeling of the system is only possible through numerical solutions. For this reason several works have used numerical models to describe experimental results [17, 18, 19].

In this work, the modeling of the signal generated by using SWV in a system compromising an electrochemical cell and a mesoporous membrane is developed to predict its behavior; the obtained results are compared with cyclic voltammetry experiments. The model is compared with experimental results obtained with a two part electrochemical cell (Figure 1) using as mesoporous membrane an alumina filter with pores of 20 nm diameter. The membrane was mechanically blocked with an insulating varnish, or chemically blocked by the adsorption of horseradish peroxidase (HRP) or avidin. The effect in mass transport due the way in which the pores are blocked is discussed, showing that when a small probe is used (less than 1 nm diameter), there are no major differences between considering either completely blocked pores or all the pores partially blocked (Scheme 1).

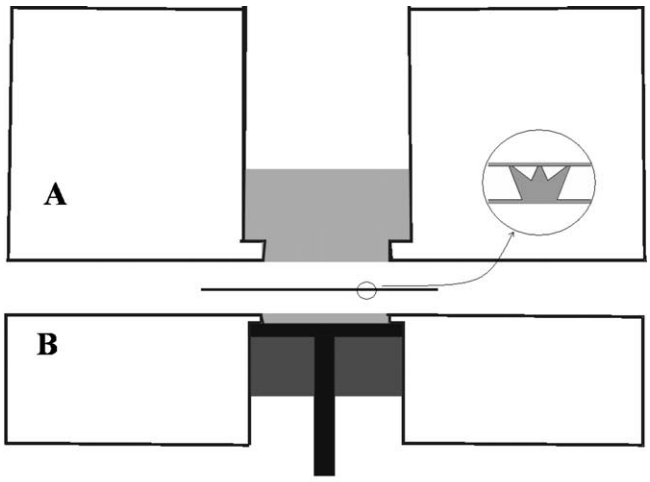

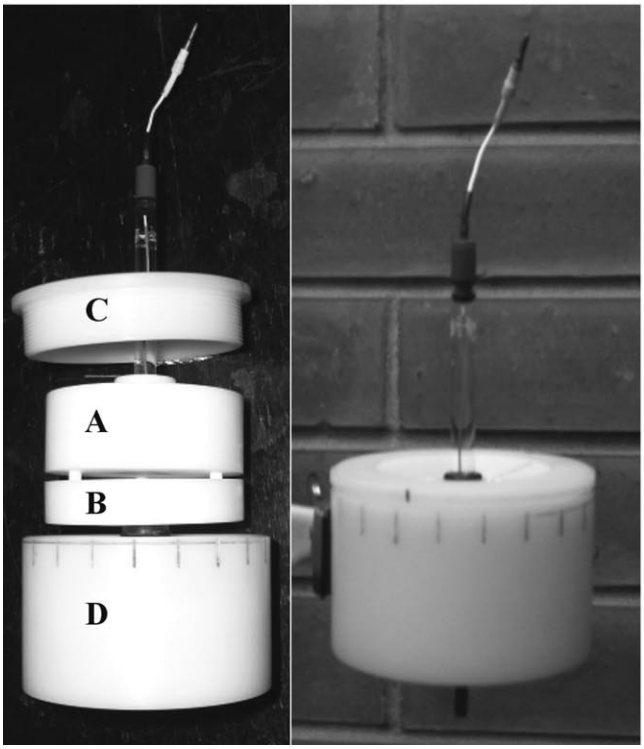

Fig. 1. Top: Scheme of the experimental cell. In black is depicted the conducting parts of the electrode, horizontally the gold surface, vertically the bronze shaft. In dark gray the insulator part of the electrode. In light gray the space occupied by the solutions. The thin line between parts A and B represents the alumina membrane. The zoom depicts the geometry given to the pores in the digital model. Bottom: Two photographs of the system: Left, A and B corresponds to the parts represented in the scheme, and C and D are the parts corresponding to the holder to maintain tight the whole system. Right, the system is assembled ready to use.

2. Experimental

2.1. Reagents and Materials

Horseradish peroxidase (HRP) was provided by Biozyme, 3-aminopropyl(triethoxy)silane (APTES), avidin from egg white, biotin-LC-hydrazide, 2-(*N*-morpholino)ethanesulfonic acid (MES), *N*-(3-dimethylaminopropyl)-*N*′-ethylcarbodiimide hydrochloride (EDC) and *N*-hydroxysuccinimide (NHS) were provided by Sigma; alumina membranes, Anodisc 25, were provided by Whatman. All other reagents were analytical grade.

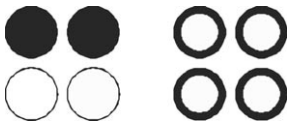

Scheme 1. Representation of the two blocking models. Both models represent a 50% of blocked pores (black). At left, the completely blocked pores model (C model); at right, the all partially blocked pores model (P model).

2.2. Membrane Modification

Mechanical modification: the alumina membrane was blocked at different extents with an electrical insulating varnish (Electroquímica Delta, Argentina).

Nonspecific adsorption: the alumina membrane was exposed at different HRP concentrations in 0.1 M phosphate buffer (pH 7.4) for 45 minutes.

Specific adsorption: The alumina membrane was immersed in a 5% APTES solution in dry toluene under stirring for one hour. The membrane is rinsed with toluene and placed in an oven at 120 °C for 20 minutes. Then, the membrane is placed in a 300 mM succinic anhydride solution in DMSO under stirring overnight. The membrane is rinsed with DMSO, acetone and water. The surface is activated with a 100 mM EDC and 100 mM NHS in 50 mM MES buffer (pH 5.5) for 30 minutes under stirring, thereafter the surface is rinsed with water and incubated with a 0.3 mM biotin-LC-hydrazine in 50mM MES (pH 5.5) for 1 hour. Then the nonmodified carboxylic groups were quenched with a 0.1 M ethanolamine solution (pH 8.5) for 15 minutes and then rinsed with water. Avidin is incubated at different concentrations in a 50 mM MES buffer (pH 5.5) for 45 minutes; then, the membrane is rinsed with buffer.

2.3. Electrochemical Cell

A two-part electrochemical cell made in Teflon was used. In the lower part, the working electrode is placed leaving a shallow cavity where a solution is introduced (Figure 1). On the top of this part, an alumina membrane is placed. Over the alumina membrane the upper part of the cell is adjusted and filled with the probe solution; then, the counter and reference (Ag/AgCl) electrodes are introduced. The complete cell is placed in a holder that keeps tight the whole system.

2.4. Electrochemical Experiments

Square wave voltammetry experiments were carried out in the electrochemical cell previously described, using gold as working electrode at the base of the cell; the porous alumina membrane is placed at specific distance from the working electrode. The gap between the working electrode and the membrane is filled with buffer; while over the membrane, the cell is filled with the electroactive probe solution, 4 or 10 mM potassium ferrocyanide solution in 0.1 M phosphate buffer pH 7.0. The probe is left to diffuse through the membrane for 100 seconds and the square wave voltammetry is run. SWV were carried out in an μAUTOLAB type III potentiostat provided with software for data acquisition. The applied parameters were: Amplitude 20 mV, frequency 25 Hz, step 5 mV. Using the same system, cyclic voltammetry experiments were carried out at a 125 mV s^{-1} scan rate.

2.5. Numerical Model

Finite-element software (Comsol Multiphysics 3.4) was used to simulate the cyclic voltammetry and square wave voltammetry experiments and the concentration profiles. The software was executed in a PC Intel Corel Duo, 4 GB RAM, Windows XP operative system, resolving the model with 241000 degrees of freedom and ca. 100000 nodes.

3. Results and Discussion

The models developed in this work correspond to the experimental set up shown in Figure 1. The electrochemical cell comprehends two parts. The upper part A contains the probe solution (in light grey), the counter and the reference electrodes (not represented); while the bottom part B contains the working electrode at a fixed distance from the top, leaving a gap where a buffer solution is placed during the experiments. The modified alumina membrane is placed between the two parts of the cell (represented by a thin line). The system is assembled and introduced inside a holder D (left photography) and closed with a screw cap C that keeps tight the system (right photography). The marks at the top of the holder are used as reference to maintain the reproducibility of the ensemble; in this way always the same pressure is applied onto the membrane, therefore the gap between electrode and membrane remains constant throughout all the experiments.

The experimental system was modeled solving Poisson and Nernst–Plank without electroneutrality equations using finite-element software to obtain the cyclic voltammetric and square wave voltammetric responses and the concentration profiles. The space dimension was set to 2D and the boundary conditions were as an infinite plane electrode and semi-infinite diffusion, and the generated current is calculated by the Butler–Volmer equation. We employed physical constants referred to the 4 or 10 mM $Fe(CN)_6^{3-}/Fe(CN)_6^{4-}$ redox couple in a solution containing 0.1 M phosphate buffer as supporting electrolyte. If the model takes into account the presence of the supporting electrolyte, the migration process is negligible. Therefore in most of the numerical experiments only diffusion was taken into account for the mass transport process, avoiding considering the presence of the supporting electrolyte, in this way an important time saving is observed for the calculations.

At $t=0$ in the gap, the concentration of redox couple is equal to 0, and in the other side of the membrane the concentration of redox couple is equal to experimental bulk concentration, buffer concentration is the same in both sides of the membrane. For $0<t<100$ s only diffusion process take place in the numerical system, and for $t>100$ s cyclic voltammetry or square wave potential is applied and the current density produced by the electroactive species is given by:

$$j = Fk_0 \times \left[C_O \exp(\frac{-\alpha F}{RT}(E-E_{eq})) - C_R \exp(\frac{(1-\alpha)F}{RT}(E-E_{eq}))\right] \quad (1)$$

where C_R and C_O are the concentration on the working electrode surface of the reduced and the oxidized species, respectively; k_0 is the standard electron transfer rate constant; $\eta = E - E_{eq}$ is the applied overpotential and E_{eq} is the equilibrium electrode potential. A value of $k_0 =$ 0.01 cm s^{-1} was employed. This value arises from the adjustment of the model to experimental cyclic voltammetries on gold. Using this value, the model is able to reproduce the peak high and the peak separation of cyclic voltammetries at different scan rates.

The square wave potential signal is characterized by a staircase potential (ΔE_s), over which is mounted a square wave with a amplitude given by the pulse height potential (ΔE_p); In the numerical model the applied potential can be represented by the following function:

$$E(t) = \frac{4\Delta E_p}{\pi}\sum_n \frac{1}{2n-1}\sin[(2n-1)2\pi\omega t + \pi] + \Delta E_s \,\mathrm{int}(\omega t) \quad (2)$$

where $E(t)$ is the applied potential at the time t. The first term represents the applied square wave and it was generated using a Fourier series containing only odd integer harmonics with the same parameters than in the experimental case; ΔE_p corresponds to the amplitude of the square wave (0.020 V); ω is the applied frequency (25 Hz); while n is the number of harmonics used, 7 in this work. The second term corresponds to the applied staircase potential (ΔE_s), where int(ωt) is a function which returns the lowest integer to ωt.

Another way to approximately represent the applied potential is using the following equation:

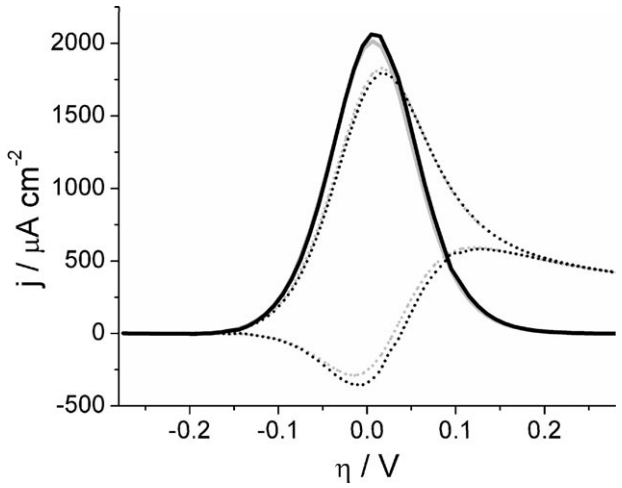

Fig. 2. Numerical simulation of square wave voltammetry. Lines in black are obtained using Equation 2, lines in grey are obtained using Equation 3. Forward and backward currents are in dotted lines. Difference current is in full line. Parameters: $\Delta E_p = 20$ mV, $\Delta E_s = 5$ mV, $\omega = 25$ Hz, $v = 0.125$ V s^{-1}, 4 mM ferrocyanide solution.

$$E(t) = \frac{4\Delta E_p}{\pi} \sum_n \frac{1}{2n-1} \sin[(2n-1)2\pi\omega t + \pi] + vt \qquad (3)$$

in the second term, the staircase potential is replaced by a continuous function, where $v = \Delta E_s/2\omega$.

Equation 2 is a better representation of the experimental SWV, however Equation 3 is more stable numerically; the numerical results obtained from each equation are presented in Figure 2, showing a minimum difference between them (ca. 2%) for the conditions used in this work; therefore in the rest of this work the numerical model using Equation 3 was used.

To validate the numerical model developed, the first step was to simulate the electrode response to a square wave voltammetry in a typical electrochemical cell without a membrane for a reversible couple, an experiment widely characterized in the literature. The obtained values were compared to the theoretical prediction of the response [14, 16]:

$$\Delta i_p = \frac{nFAD^{1/2}C^*}{\pi^{1/2}t_p^{1/2}} \Delta\psi_p \qquad (4)$$

where t_p is the pulse time width, F is the Faraday constant, A is the electrode area, D and C^* are the diffusion coefficient and the bulk concentration for the electroactive species, and $\Delta\Psi_p$ is a factor that depends on the staircase step height potential (ΔE_s), the pulse height potential (ΔE_p), and the number of exchanged electrons (n). These values are reported for different conditions; i.e. for $n = 1$, $\Delta E_s = 5$ mV and $\Delta E_p = 20$ mV, $\Delta\Psi_p$ is 0.4686. Considering these values, an area of 1 cm^2, and given the concentration and the diffusion coefficient for the electroactive species a peak current, Δi_p, can be predicted. As an example, considering ferrocyanide solution with a $D = 6.5 \times 10^{-6}$ cm^2 s^{-1} and $C^* = 4$ mM, the values obtained for Δi_p are 1.989 mA, using Equation 4 and 2.000 mA using the numerical model developed in this work, a difference smaller than 1%.

Once the numerical representation of the SWV was validated with the theory, the next step was to model the system introducing the mesoporous membrane. As in a previous work [9], the system was modeled leaving a 650 μm gap between the working electrode and the membrane. The physical characteristics of the membrane are established using the information given by the supplier (thickness: 60 μm, hole diameters: 20 and 200 nm on each side, and porosity 25–50%) plus the structure information given by scanning electron microscopy [9]. In Figure 1 top, the zoom placed on the membrane shows the geometry used to represent their pores; a crown with a 200 nm base and three peaks with 20 nm width at the top. The membrane behaves as a barrier between the electrode and the probe, therefore its distance to the electrode will introduce an important effect on the concentration profile. Figure 3 shows the concentration profiles for the probe after 100 seconds of diffusion and at three different potentials for two different gaps. The distances selected are 100 and 650 μm; for the first one (Figure 3a), it can be observed a sharp change in the concentration profile as the potential is scanned to more positive values, going beyond the membrane. In the case of 650 μm, the profile change is less pronounced, and in the time period of the electrochemical experiment, the concentration profile close to the membrane is practically constant. The position of the membrane produces several effects, one hand as the membrane is closer to the electrode, the peak current observed is higher, but at the same time the membrane is involved in the electrochemical process, it can act as a resistance and eventually produce a distortion in the signal [20]. When the membrane is placed at a distance of 650 μm, the changes in the concentration profile during the electrochemical process (Figure 3b) are negligible at the vicinity of the membrane. Also, it has the experimental advantage that small changes in the distance between membrane and electrode have not major effects in the concentration profile, and the peak currents can still measured with high precision as we will see further in this work.

In Figure 4 are compared the response to CV and SWV for the same solution using conditions in which the potential scan rate is the same in both experiments (125 mV s^{-1}). It is worth mentioning that in the case of cyclic voltammetry, the scan rate used corresponds to an experimental condition in which an important background current may be observed, depending of the characteristics of the electrode and the ohmic drop introduced by the membrane; while for SWV the used conditions corresponds to a frequency of 25 Hz, a situation in which ferrocyanide shows a reversible behavior. The ratio between SWV and CV peak currents ($\Delta i_p/i_p$) is 2.25; this value is a constant if both experiments are carried out using the same time frame to scan the potential, showing

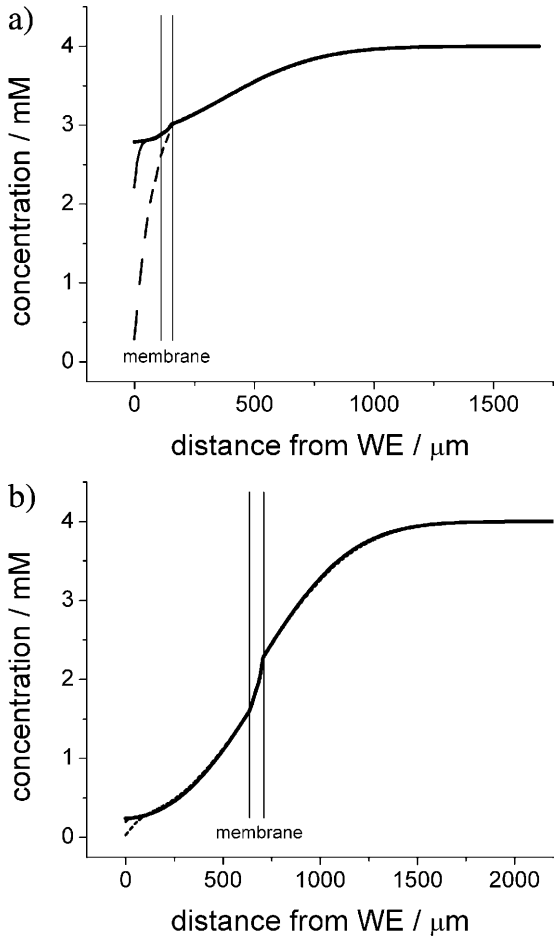

Fig. 3. Numerical quantitative concentration profiles of $Fe(CN)_6^{3-}$ with a membrane placed from the working electrode at (a) 100 μm and (b) 650 μm. The profiles are evaluated at $\eta = -0.275$ V (bold line), 0 V (thin line) and 0.275 V (dashed line). SWV conditions idem Figure 2.

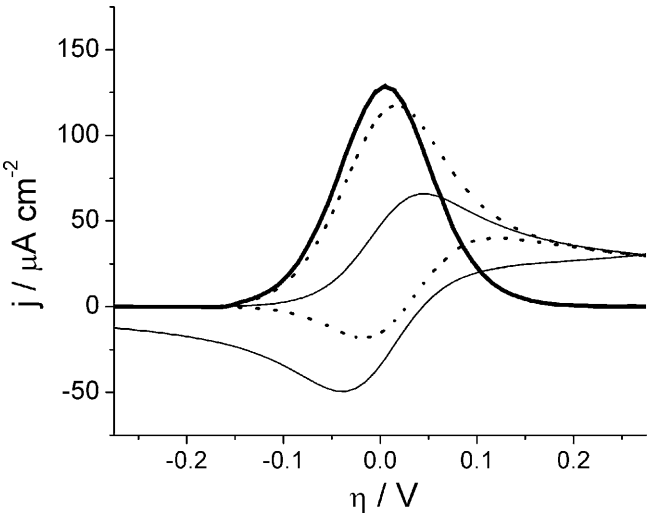

Fig. 4. Numerical simulations of cyclic voltammetry (thin line) and square wave voltammetry (bold line) for a 4 mM ferrocyanide solution. Membrane-electrode gap: 650 μm. CV scan rate: 0.125 V s^{-1}. SWV conditions idem Figure 2. In dotted lines the forward and backward currents obtained for the SWV.

the better sensitivity of SWV. Another aspect to take into account is the fact that background current in CV remains practically constant at any concentration of the electroactive species, therefore if a lower probe concentration is used, the signal/noise ratio gets worse; while for SWV this problem is almost suppress. This is particularly important if molecules with low solubility are planned to be used, as on purpose synthesized macromolecules containing a redox moiety to study the effect of the probe molecular size in this type of sensors.

Considering the experimental parameters for SWV, the response of a partially blocked membrane was studied by painting sections of the membrane with an insulating varnish. Peak currents were measured per duplicate, assembling and disassembling the whole system, showing differences between measurements less than 10%, that can be considered a very good performance for an electrochemical system [21, 22]. At the same time, it was simulated its behavior. Figure 5 shows experimental and numerical results obtained for a system compromising a blocked membrane at 650 μm distance from the working electrode. The numerical data (circles) generated with the proposed model presents a good agreement with the experimental results (stars).

From the point of view of an analytical application, as the concentration of the analyte increases, the remaining free pores decrease and, therefore the signal decreases. In order to obtain a direct relationship between signal and analyte concentration, we define the analytical response, $R(f)$, as:

$$R(f) = \frac{i_{p,1} - i_{p,f}}{i_{p,1}} \quad (5)$$

where f represents the fraction of free pores; $i_{p,1}$ is the peak current obtained with the membrane has all the pores free, and $i_{p,f}$ is the peak current obtained with a remaining fraction of free pores (f), that in turn corresponds to a given concentration of analyte. R is a function that scales from 0 to 1, with 1 indicating that the surface is completely blocked. In this way the function is a very simple indicator of the sensitivity of the system to detect an analyte. For example, if at a low analyte concentration a value of R close to 1 can be obtained, this means the system is very sensitive. Figure 6 shows the plot of the analytical response R as a function of the remaining free pores using the numerical data obtained previously (Figure 5), showing a perfect fit if the fraction of free pores is plotted in a logarithmic scale.

Although the blocking of the surface using an insulating varnish is a simple and straightforward method to check the ability of the model to describe experimental data, from a chemical point of view the idea of some pores completely blocked and other completely free may not correspond to a real experiment, and it is more likely that all the pores are partially blocked. For this reason two numerical models representing the blocked pores were developed (Scheme 1),

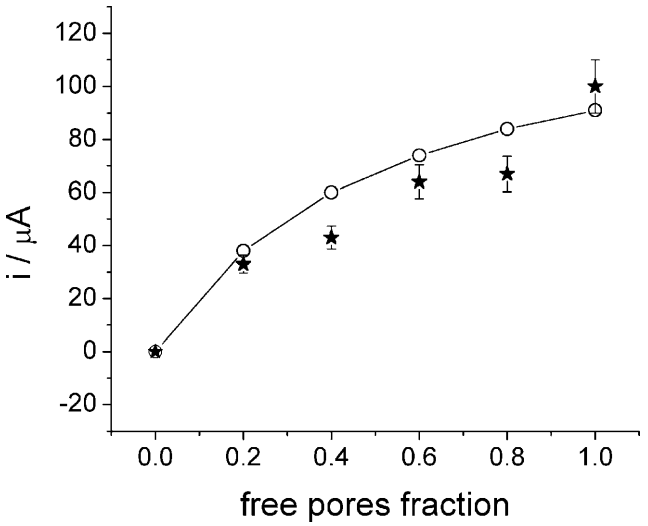

Fig. 5. SWV peak current as a function of the remaining free pores fraction. Circles: numerical data, asterisks: experimental data. Membrane-electrode gap: 650 μm, ferrocyanide bulk concentration: 4 mM. Electrode area: 0.735 cm^2. SWV conditions idem Figure 2.

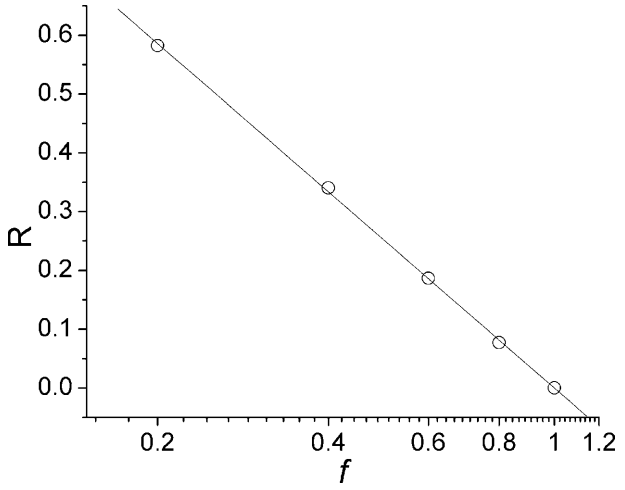

Fig. 6. Analytical response, *R*, as function of free pores fraction represented in logarithmic scale. *R* values are calculated from the numerical data represented in Figure 5.

one, already presented, considering a fraction of completely blocked pores (C model, left in the scheme), and the other considering that all the pores are partially blocked (P model, right in the scheme).

Figure 7 shows the behavior expected for both models. Taking into account that a probe with less than 1nm diameter is used [23], the size effect of the pores on the way the molecule diffuses is only important when it is almost completely blocked, therefore it can be expected that differences between the two models can only be observed at low fraction of free pores. In the figure is also considered the typical standard deviation in an electrochemical experiment, showing that differences between both models begin to be observed when the free pore fraction are less than 0.4

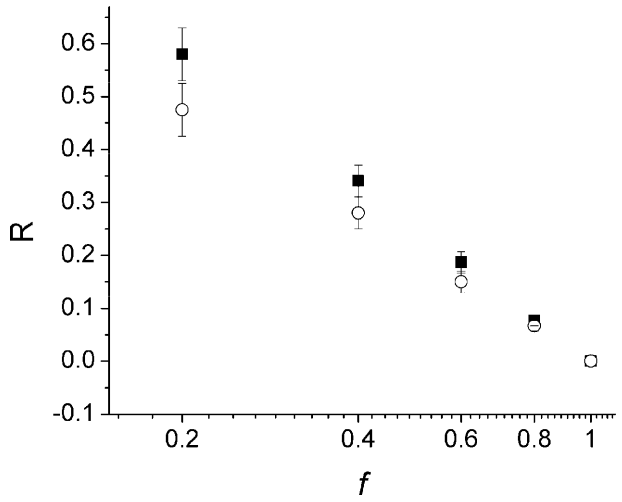

Fig. 7. Analytical response as a function of free pores considering two different models to block the pores. Squares: fraction of completely blocked pores (C model), circles: all the pores partially blocked (P model).

and are really significant when the fraction of free pores reaches 0.2.

Finally, the numerical model is tested with two real experimental systems, a first one using horseradish peroxidase (HRP) that can be adsorbed nonspecifically onto alumina membranes and the other one using the system biotin-avidin in which avidin is adsorbed onto a biotin modified membrane through a specific recognition reaction. HRP is an elongated protein, with long and short axes ca. 6.4 and 3.7 nm, respectively [24]; while avidin can be considered globular protein with 6.2 nm diameter [25]. The analytical responses *R* for both systems are depicted in Figure 8, it can be observed that both analytes arrives to a plateau relatively at low concentrations; however the value of *R* does not exceed 0.6.

The *R* values presented in Figure 8 can be related to the remaining free pores (*f*) using the calibration curve presented in Figure 6, that in turn allows to relate the remaining free pores with the analyte concentration (Figure 9). These results show that even though the surface is saturated with the analyte, an effective free pore area is still present allowing the diffusion of a small molecule as ferrocyanide.

4. Conclusions

Our results shown that digital simulation of square wave voltammetry using finite element algorithms can accurately predict the amperometric response of an electroactive species, and be applied to the design of mesoporous membrane based sensors. Experimentally, the designed electrochemical cell is easy to handle, and reproducible results can be obtained.

The relative change in current due to the decrease of free pores in the membrane was defined as analytical response *R* and follows a logarithmic behavior; this allows predicting

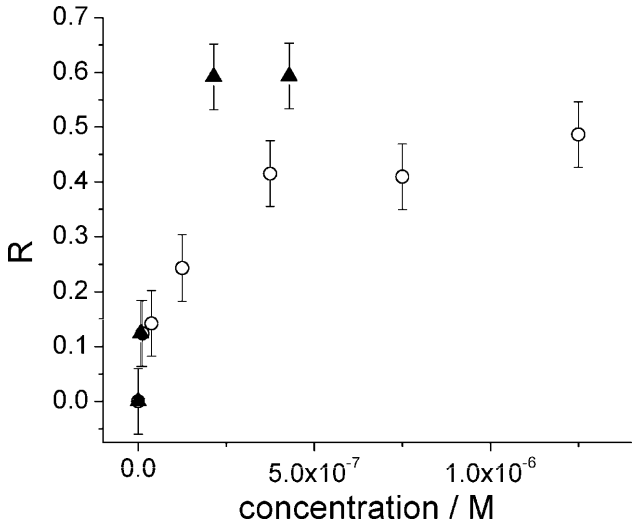

Fig. 8. Analytical response of the alumina membrane to HRP (circles) and avidin (triangles). All the determinations were carried out by duplicate.

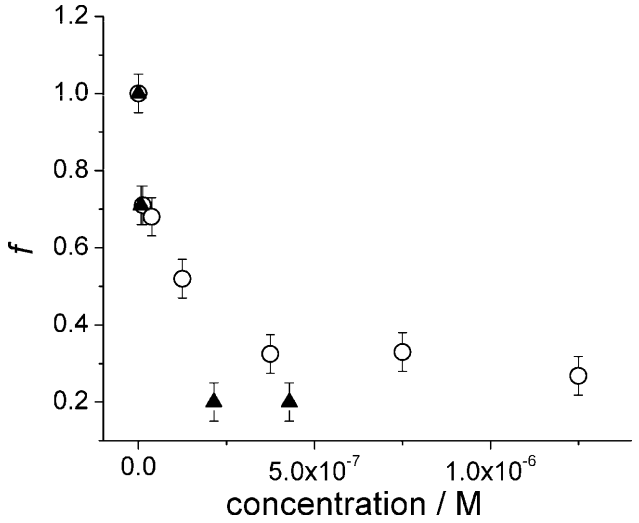

Fig. 9. Remaining free pores as a function of protein concentration. Circles: nonspecific adsorption of HRP; triangles: specific adsorption of avidin.

the conditions in which the system will be sensitive enough to overcome the experimental error. Considering the variability of the results in electrochemical experiments [21, 22], it is important that the change in the signal be greater than 10% to have a statistical significance. The results plotted shows that at least a 25% reduction of free pores has to be produced to obtain a 10% current change ($R = 0.1$) in this type of membrane. Also, the simulation allows to observe the importance of a significant coverage of the surface, since even when only 20% of the pores remains free ($f = 0.2$) the value of R is ca. 0.6. This result suggests the system membrane/analyte/probe has to be redesigned to improve the sensitivity of the device.

The sizes of the pore, the analyte and the probe are key parameters in the development of this type of sensors. In this work, we have developed our simulated system modeling the behavior of a commercial available membrane with pore size of 20 nm; while the probe diameter is considered negligible in our model, experimentally ferrocyanide, an ion with less than 1 nm, has shown to behave very close to the predictions of the model. Finally, the blocking of the pores were simulated in two different ways (models C and P, Scheme 1); experimentally were tested either blocking completely a fraction of the pores with an insulating varnish (C model), or blocking partially all the pores (P model) by adsorption of chemical species. In the first case, as the varnish does not allow the diffusion of the probe from one compartment to another, a complete blocking of the system can be obtained. The same result cannot be obtained by chemical modification in the conditions used in this work. In this case, molecules with an average diameter of 6 nm randomly cover the membrane, and also the affinity of the analyte for the surface should be taken into account. Comparing avidin with HRP, the signal saturation is observed at lower concentrations for the former, and the value of R is greater (Figure 8); this result can be attributed to the high affinity of biotin modified membrane toward avidin. In this case an R, close to 0.6 is achieved representing a free pore fraction ca. 0.2; while for HRP, R is ca. 0.5, representing a free pore fraction around 0.3 (Figure 9). These results suggest that even at a high coverage a small probe can easily diffuse through the small gaps left between the adsorbed molecules, decreasing the sensitivity of the method. Another point to take into account is the alumina surface selectivity, a problem similar to the one observed on gold surfaces. We consider it can be solved modifying the surface with a PEG derivative, a dextran derivative or a mixture of both, as our group has previously done with gold surfaces [26]. The introduction of this type of coverage will not introduce important changes in the diffusion process through the membrane as they are open structures plenty of water.

Numerical experiments have demonstrated to be a successfully tools in other scientific areas to save time and money. In this case, it allows us to design an experimental cell knowing that the selected electrode-membrane gap, plus other parameters, can achieve current values able to be measured with a conventional potentiostat. It makes us realize of the logarithmic relation between response and free pores, a fact that it cannot easily predicted, and also it allows to easily study the effect of different variables (pore density, pore size, distance electrode-membrane, electrochemical technique and parameters, etc.) previous to an experimental confirmation. The effect on the assay development for a given analyte is relevant, since it can be numerical tested the effect of different membranes, to see which of those experimentally available can achieve the desired detection limit. Another way to see the same problem is looking for the ideal membrane, and once it is found, sees if it is possible to produce it. In the future, as the model will be refined, other parameters as probe size, non specific adsorption, and others could be also analyzed.

Acknowledgements

ANPCyT (PICT 00575) and *Universidad de Buenos Aires* (X012, X850) are acknowledged for financial support. GG and FB are *CONICET* research staff members.

References

[1] F. Breton, R. Rouillon, E. V. Piletska, K. Karim, A. Guerreiro, I. Chianella, S. Piletsky, *Biosens. Bioelectron.* **2007**, *22*, 1948.
[2] Y. Lv, Z. Lin, T. Tan, W. Feng, P. Qin, C. Li, *Sens. Actuators B* **2008**, *133*, 15.
[3] E. V. Piletska, M. Romero-Guerra, I. Chianella, K. Karim, A. P. F. Turner, S. A. Piletsky, *Anal. Chim. Acta* **2005**, *542*, 111.
[4] V. Flexer, M. V. Ielmini, E. J. Calvo, P. N. Bartlett, *Bioelectrochemistry* **2008**, *74*, 201.
[5] P. N. Bartlett, K. F. E. Pratt, *J. Electroanal. Chem.* **1995**, *397*, 53.
[6] S. Lee, Y. Zhang, H. S. White, C. C. Harrell, C. R. Martin, *Anal. Chem*. **2004**, *76*, 6108.
[7] C.-C. Chen, M. A. Derylo, L. A. Baker, *Anal. Chem.* **2009**, *81*, 4742.
[8] E. N. Ervin, R. J. White, H. S. White, *Anal. Chem.* **2009**, *81*, 533.
[9] G. González, G. Priano, M. Günther, F. Battaglini. *Sens. Actuators B.* **2010**, *144*, 349.
[10] Z. Siwy, L. Trofin, P. Kohli, L. A. Baker, C. Trautmann,C. R. Martin, *J. Am. Chem. Soc.* **2005**, *127*, 5000.
[11] I. Vlassiouk, P. Takmakov, S. Smirnov, *Langmuir* **2005**, *21*, 4776.
[12] B. Zhang, Y. Zhang, H. S. White, *Anal.Chem.* **2004**, *76*, 6229.
[13] J. Dai, G. L. Baker, M. L. Bruening, *Anal. Chem.* **2006**, *78*, 135.
[14] A. J. Bard, L. R. Faulkner, *Electrochemical Methods: Fundamentals and Applications*, 2nd ed, Wiley, Chichester **2001**, pp. 293.
[15] J.Osteryoung, J. J. O'Dea, *J. Electroanal. Chem.* **1986**, *14*, 209.
[16] J. H. Christie, J. A. Turner, R. A. Osteryoung, *Anal. Chem.* **1977**, *49*, 1899.
[17] V. Mirceski, S. Skrzypek, M. Lovric, *Electroanalysis* **2009**, *21*, 87.
[18] M. Rudolph, *J. Electroanal. Chem*. **2001**, *503*, 15.
[19] N. Fatouros, D. Krulic, *J. Electroanal. Chem*. **1998**, *443*, 262.
[20] V. Mirčeski, M. Lovrić, *J. Electroanal. Chem*. **2000**, *497*, 114
[21] G. Priano, G. Gonzalez, M. Günther, F. Battaglini, *Electroanalysis* **2008**, *20*, 91.
[22] C-Y. Lee, Y-J. Tan, A. M. Bond, *Anal. Chem.* **2008**, *80*, 3873.
[23] H. J. Buser, D. Schwarzenbach, W. Petter, A. Ludi, *Inorg. Chem*. **1977**, *16*, 2704.
[24] H. Takahashi, B. Li, T. Sasaki, C. Miyazaki, T. Kajino, S. Inagaki, *Chem. Mater.* **2000**, *12*, 3301.
[25] A. B. Kharitonov, J. Wasserman, E. Katz, I. Willner, *J. Phys. Chem. B* **2001**, *105*, 4205.
[26] D. Pallarola, L. Domenianni, G. Priano, F. Battaglini, *Electroanalysis* **2007**, *19*, 690.